FAILURE MECHANISM OF KAMAISHI BREAKWATERS DUE TO THE GREAT EAST JAPAN EARTHQUAKE TSUNAMI

Taro Arikawa[1], Masaharu Sato[2], Kenichiro Shimosako[3], Iwao Hasegawa[4],

Gyeong-Seon Yeom[5] and Takashi Tomita[6]

Many breakwaters were damaged by the Great East Japan Earthquake of March 11, 2011. The majority of the breakwaters were destroyed or deformed under tsunami overflow; however, the failure mechanism under tsunami overflow is not clear. Therefore, with the main objective of this report being to clarify the stability of breakwaters under tsunami overflow, hydraulic model experiments and numerical simulations were conducted with Kamaishi Bay breakwaters as the subject, and failure mechanisms of the trunk of the breakwaters were examined.

Keywords: Kamaishi breakwater; tsunami overflow; stability of breakwaters

INTRODUCTION

The tsunami caused by the Great East Japan Earthquake collapsed many breakwaters and storm surge barriers. Views of this were recorded by video cameras at many places, and in many cases, it is presumed that the tsunami exceeded the heights of the breakwater etc., causing their failure.

Among past studies focused on clarifying the mechanism of the failure of breakwaters caused by tsunami, Horiguchi and Yokota (1968) investigated the causes of the failure of the Kawaragi Breakwater in the Port of Hachinohe when it was struck by the Tokaichi Earthquake tsunami, reaching the hypothesis that it slid under the impacts of the water level difference inside and outside the port and the dynamic water pressure on its front surface. Tanimoto et. al. (1983) suggested that the failure of the landfill revetment then under construction in the outer harbor of Noshiro during the Japan Sea Chubu earthquake tsunami was a failure caused by the impact of a bore tsunami.

But there has been no research on the stability of breakwaters when a certain period of time has elapsed after overflow, as occurred during this recent tsunami. So this research took Kamaishi as an example to perform hydraulic model experiments and numerical simulations of trunks of breakwater, in order to clarify the breakwater failure mechanism under tsunami overflow.

Photo 1. The Kamaishi Bay mouth breakwaters (taken by Tohoku Regional Bureau)

[1] Coastal and Ocean Engineering Field, Port and Airport Research Institute, 3-1-1 Nagase, Yokosuka, Kanagawa, 239-0826, Japan
[2] Coastal and Ocean Engineering Field, Port and Airport Research Institute
[3] Coastal and Ocean Engineering Field, Port and Airport Research Institute
[4] ECOH CORPORATION, 2-6-4 Kitaueno, Taito-ku, Tokyo, 110-0014, Japan
[5] Asia-Pacific Center For Coastal Disaster Research, Port and Airport Research Institute
[6] Asia-Pacific Center For Coastal Disaster Research, Port and Airport Research Institute
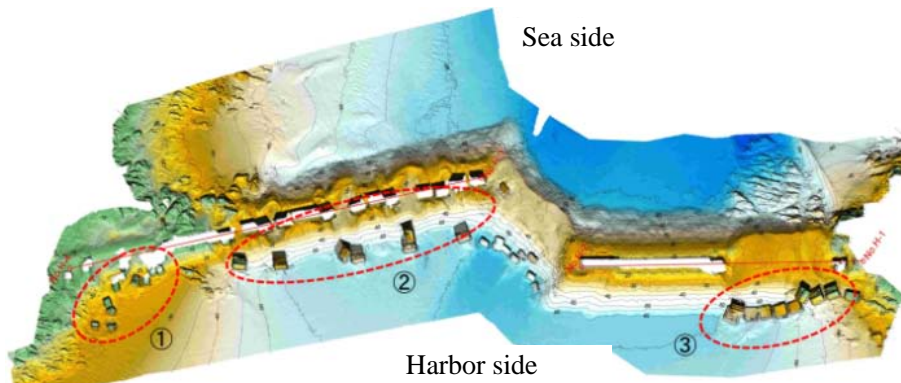
STATE of STUDIES of FAILURE MECHANIM of KAMAISHI BAY MOUTH BREAKWATER

State of the Kamaishi Bay Mouth Breakwaters

The Kamaishi Bay mouth breakwaters include the North Breakwater (length 990m), South Breakwater (length 670m), and the Bay mouth section (length 330m) as shown in Photo 1. The maximum depth at the breakwaters is 63m.

At the North Breakwater, the deep section consists almost entirely of trapezoidal caissons shown in Fig. 1., and its foundation mound ranges from -60m to -27m, and above it, caissons weighing about 36,000 tons are installed. In shallow parts, the caissons are rectangular with height ranging from 10m to 15m. At the South Breakwater, 3 caissons are, as in the North Breakwater, trapezoidal caissons, and the rest are approximately 32,000 ton rectangular caissons. Their crest height is D.L. +6.0m (T.P. +5.14m), and their foundation mound extends from depth of -55 to depth of -22m. At the mouth section, a submerged breakwater has been built, the depth at the mouth is D.L. -19.0m, and armor blocks are inserted around it.

Figure 1. Cross Section of Kamaishi Breakwater at Deep Area of North Side

State of damage of the Kamaishi Bay Mouth Breakwaters

Fig. 2. shows caissons which slid and leaned according to the results of a survey by the Tohoku Regional Development Bureau. On the North Breakwater, out of 22 caissons in the deep part, 7 slid, 14 leaned, and 1 was undamaged. And as the figure shows, they slid just like teeth falling out. In the shallow part, out of 22 caissons, 11 were pulled out, 5 leaned, and 6 were undamaged. And of the 6 which were undamaged, mats were installed on 5 to increase friction. At the mouth, out of the 13 caissons of the submerged breakwaters, only 1 remained, because the rest had slid. At the South Breakwater, out of 19 caissons in the deep part, 8 had slid, 1 leaned, and 10 were undamaged, while in the shallow part, 2 had slid and 1 leaned.

Figure 2. State of damage of Breakwater（Red : No damage, Yellow : Tilted, White : Sliding down）

Fig. 3. shows the state of damage to all the breakwaters, Photo 2. shows the state of damage to caissons near the crest of the North Breakwater, and Fig. 4. shows the detailed state of sliding of the caissons in the deep part of the North Breakwater. This shows that in the deep part at the North Breakwater, many of them slid without leaning after sliding. And Fig. 5. shows the difference between the sections before and after the disaster. On the North Breakwater, the mound was scoured from 5m to 10m.

It shows that on both the North Breakwater and South Breakwater, the toe of the slope of the mound on the inside of the bay was not seriously deformed and the caissons slid on the mound. These facts suggest that the caissons could have been gently pulled back inside the bay

Sea side

Harbor side

Figure 3. State of damage of breakwater

Photo 2. State of damage of North Breakwater

Figure 4. State of damage of North Breakwater
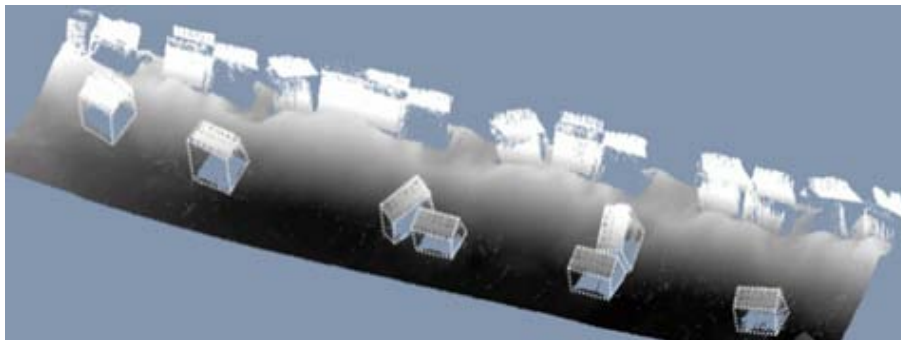
Sea side   Harbor side
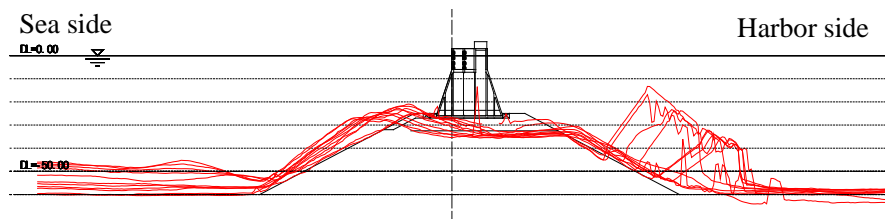

Figure 5. Cross section of damage of North Breakwater

Past Studies of Failure Mechanism of Kamaishi Breakwater

   Takahashi et al. (2011) studied the state of damage to the breakwater at the mouth of Kamaishi Harbor by using a narrow multi-beam to show the state of the sea bottom land form in detail and performing numerical simulations of Kamaishi Harbor. At that time, they studied the state of sliding of the breakwater using the water level difference obtained by numerical simulation and video images, and when they calculated the horizontal force of the water level difference inside and outside the harbor based on the numerical simulation, they calculated the sliding safety factor of the breakwater at 1.19 in deep parts and as 0.95 in shallow parts. During their study, from the video images, they observed a fast

flow at the caisson joints, estimating that scouring of the foundation mound triggered by a fast flow at the joint was the major causal factor.

Arikawa et al. (2012) performed scale 1/60 hydraulic model experiments and sliding experiments of the breakwater in deep parts, hypothesizing that sliding occurred as a result of an increase of horizontal force, because in addition to horizontal force caused by the water level difference, the front surface wave pressure was a little larger and the back surface wave pressure a little smaller than the hydrostatic pressure. And regarding the scouring of the joint, there is a high possibility that the flow velocity high enough to cause scouring did not occur, and that judging from the state of overflow scouring in the experiment, they surmised that at Kamaishi, the impact of overflow scouring was small.

Failure Causal Factors Considered

First the water level outside the harbor is raised by the tsunami, then either overflow or inflow through an opening in the breakwater raises the water level inside the harbor, and finally the tsunami is washed back from outside the harbor. This action is repeated.

A breakwater on the other hand, consists mainly of a foundation riprap and caissons, and if, under external force, sliding, overturning, and bearing capacity failure do not occur, it remains without any deformation. Sliding occurs when the external force has acted almost horizontally, and overturning is caused by large moment, so it tends to occur when the caisson is light and the water level at the back surface is low. Under such circumstances, if the bearing capacity of the foundation riprap is small, the caisson will be deformed in such a way that it sinks down into the foundation riprap (Kobayashi et. al., 1987). In this way, there are three failure modes, but it is hypothesized that in almost all cases, even failure caused by tsunami, it is failure caused by sliding mode.

The failure causes considered are as follows.

[1] Dynamic water pressure as wave force

[2] Water level difference between the outside and inside of the harbor

[3] Scouring of the foundation mound caused by overflowing and joint flow velocity

[4] Decline of bearing capacity caused by increase of pore water pressure

Assuming that during overflow, [1] is small, hydraulic model tests were done to study [2] and [3] in particular (see Fig. 6).
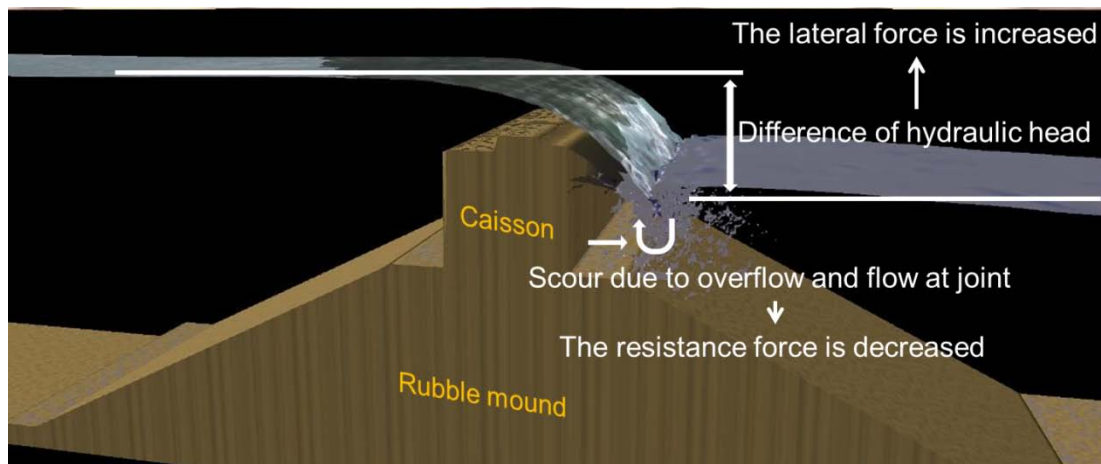

Figure 6. Major failure causal factors under tsunami overflow

HYDRAULIC MODEL EXPERIMENTS

Experiment Model

Fig. 7. is a full section diagram of the experiment. The model scale was 1/20 for the deep part at Kamaishi. A wave meter was attached as shown in the figure. The model was installed inside an approximately 70m section in the circulation device. The foundation mound was installed so that the heights of the crests of the caissons were aligned at 3.7m. The numbers in the diagram show distances from the reference line. The shapes of the caissons were trapezoidal used in the deep part and rectangular (Fig. 8.). The height of the trapezoidal caisson was 1.65m and that of the rectangular caisson was 1.4m. Wave meters (PG) were attached to the front, back, and top surfaces, while pore water pressure meters (UG) were attached to the bottom surface. The caissons were both 1.5m wide. The channel width was 3.5m, so the 1.5m wide caissons were installed in the center, and 0.9m wide dummy caissons were installed at both ends. The trapezoidal and rectangular 1.5m wide caissons

weighed 4.5m tons and 4.0 tons respectively. The trapezoidal and rectangular dummy caissons weighed 3.0 tons and 2.6 tons respectively. The weight per 1m of the dummy caissons was increased 10%. The joints were 2.5cm wide.
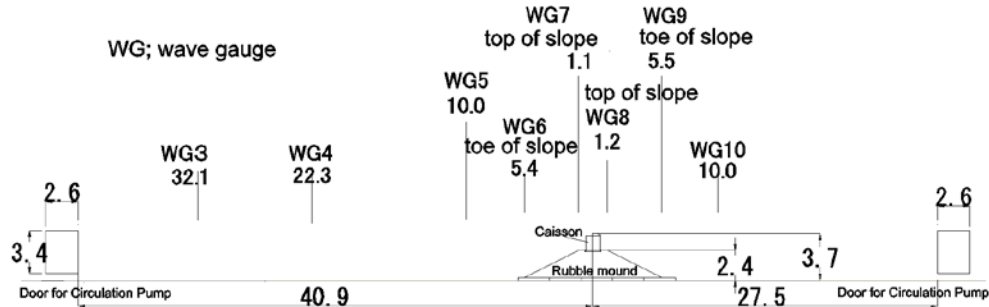

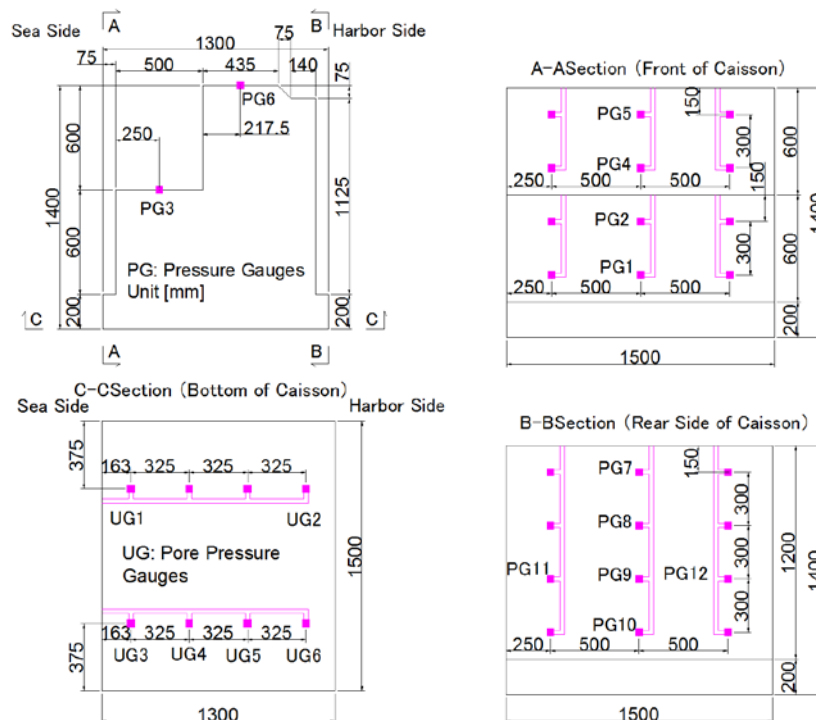**Figure 7. Experimental cross section (rectangular case, unit m)**

Figure 8. Position of pressure gauges(rectangular model, unit mm)

Experiment Cases

The experiments were performed by discharging water from the offshore side gate of the circulation device (left side of Fig. 7) and taking in the water from the shore side gate (right side of Fig. 7), creating a water level difference between the outside and inside of the harbor to simulate the state of overflow by a tsunami. The pump output was adjusted to match the water level difference and the water levels at the actual site as closely as possible. Table 1 shows the experiment cases. The experiment was done three times for each water level difference, with the water level slightly low the first two times to study the state of the mound, then the third time, the water level difference set was that assumed to exist if the caissons slid. The first water level was 3.85m for all cases. Rubble No. 3 is site conversion of about 600kg, and rubble No. 6 is site conversion of about 10kg. At Kamaishi, rubble between 10kg and 800kg were used, so three cases were set to compare differences depending on the size of the rubble.

Table 1 Experimental conditions						
Case No.	Trial	Initial water Depth (m)	Size of rubble mound	Water level of Sea Side (WG5, m)	Water level of Harbor Side (WG10, m)	Water level difference (m)
1	1		3 (average 600kg in proto type)	0.040	-0.770	0.117
	2			0.078	-0.154	0.232
	3			0.214	-0.391	0.605
2	1	3.85	3	0.080	-0.155	0.235
	2			0.111	-0.220	0.331
	3			0.213	-0.382	0.595
3	1		6 (average 10kg in proto type)	0.038	-0.064	0.102
	2			0.080	-0.150	0.230
	3			0.209	-0.398	0.607

Experiment Results

a) Views during the experiment and after the experiment

Photo 3. shows views of the third experiment in Case 1. It shows that as the water level difference was gradually increased from the initial water level, the impact of the overflow in the rear increased, the final state is the state after the caissons are pulled out, and when they were pulled out, the water level difference began its recovery. The caisson which can be observed from the window is the dummy caisson, so its weight is about 10% heavier and it did not slide.

Photo 4 to Photo 6 shows views before and after the third experiment in all cases. Because the water level difference is reduced by the pulling out of the main caissons, the distance it is displaced is shortened, and as shown by Arikawa et al., (2012), it did not slide to the bottom of the mound. The results of an in-site survey show that because the caisson slid to the bottom of the mound, it is possible that force sufficient to move the caisson for a long period of time acted. And even in case 3 where the mound was a small quantity of riprap, no traces of scouring of joints were seen. Observations during the experiments failed to show that the overflowing water mass caused scouring severe enough to reach the back toe of the caissons.
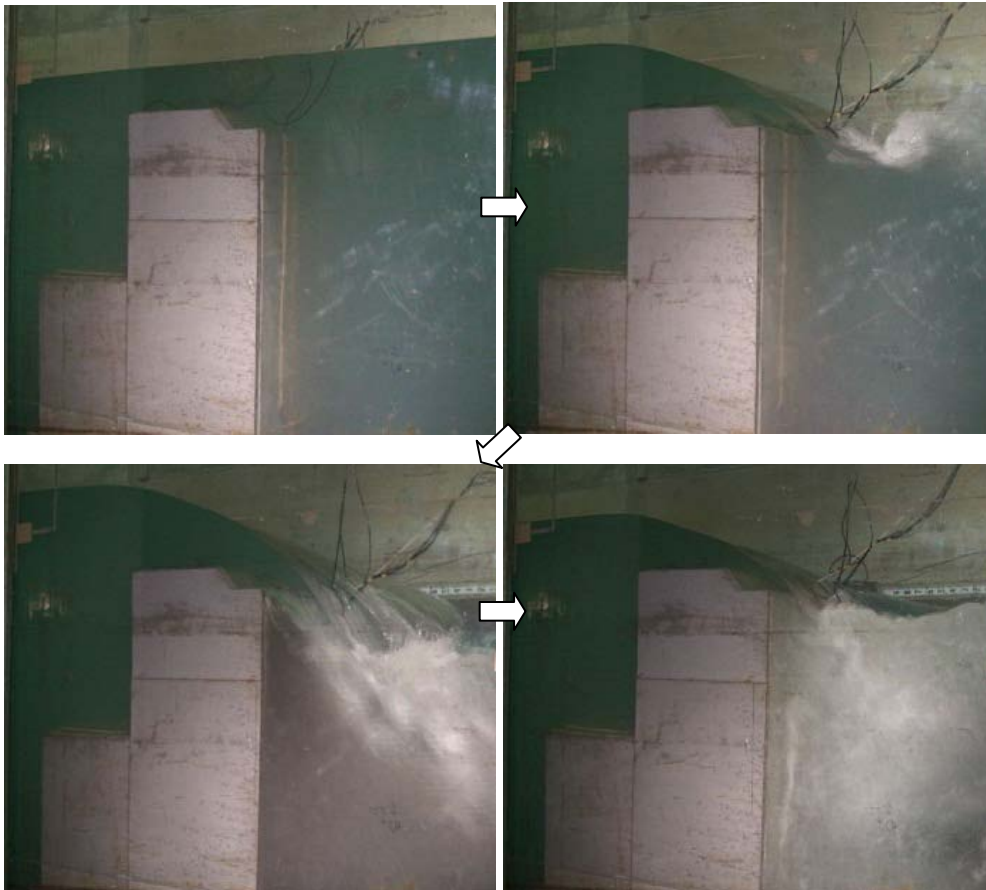

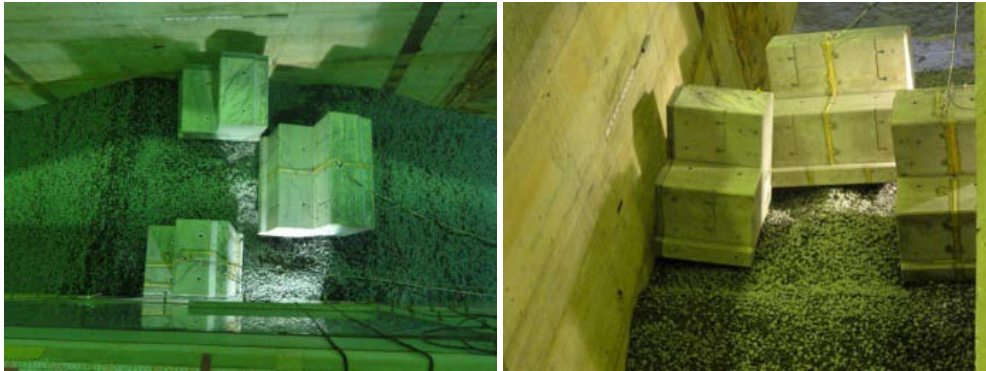**Photo 3. State of experiments (case 1 trial 3)**

Photo 4. State of breakwater After Experiments (case1 trial 3)

Photo 5. State of breakwater After Experiments (case2 trial 3)

Photo 6. State of breakwater After Experiments (case3 trial 3)

b) Joint flow velocity and sliding safety factor results

The flow velocity at joints was about 3.0m/s at the maximum water level difference in case 3, and when compared with $\sqrt{2g\Delta h}$ calculated using the water level difference Δh, it was almost equal at about 0.9 times.

Next, Table 2 shows the results of calculating the sliding safety factor based on the wave pressure in each case. An example of the sliding safety factor shown is a value when it was assumed that the friction coefficient was 0.6, and the example of the friction coefficient is the coefficient when it is assumed that the sliding safety factor was 1.0. This suggests that displacement occurs at almost 0.6, and that he sliding mode was dominant. And it also shows there are no differences resulting from the quantity of riprap.

Table 2. Sliding Safety factor and apparent friction coefficient		
Case	Sliding Safety Factor	Apparent Friction coef.
1	1.02	0.59
2	1.06	0.56
3	1.05	0.57

c) Results of wave pressure

Arikawa et al. (2012) pointed out that during overflow, wave pressure on the front surface is a little higher than hydrostatic pressure, and the wave pressure on the back surface falls to about 10% below hydrostatic pressure at the back surface water level.

And this experiment also confirmed that the front surface wave pressure is almost unchanged from the hydrostatic pressure, failing to reach a few percentage points. On the other hand, the water level at WG10 was used to study the back surface wave pressure as a percentage of the hydrostatic pressure. If the pressures at each point on the back surface are integrated by a typical surface area and the average rate of reduction is represented by Cb, the third time series in each case are as shown in Fig. 9.

Fig. 10. plots the smallest value obtained after moving averaging at 0.5s of the rates of reduction for all experiments in all cases. The axis of abscissas represents the height of the water surface above the caisson crowns. As it clearly shows, the overflow quantity increases at the same time as it falls to a maximum of about 6% of the hydrostatic pressure on the rear surface.
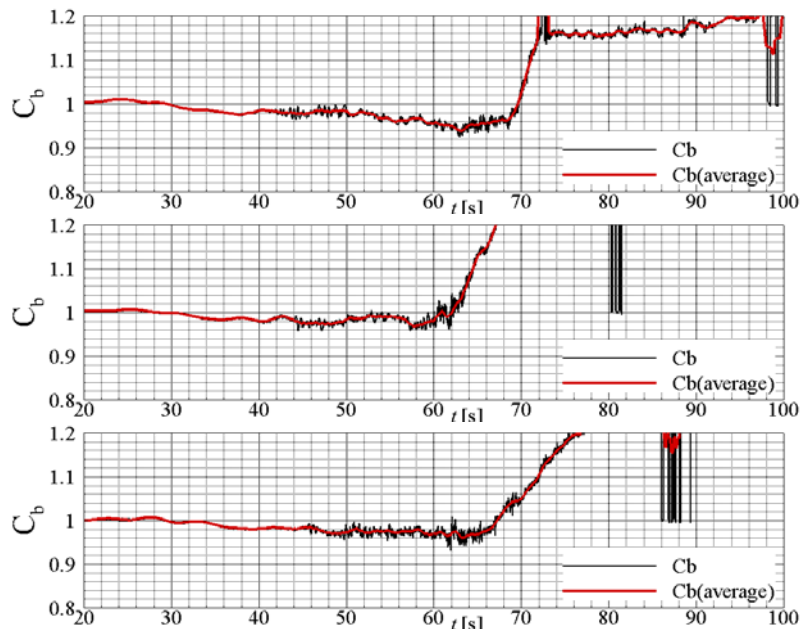
Figure 9. Time histories of the average rate of reduction (Top case 1, middle case 2, bottom case 3, red line is represented as the line, which is smoothed with moving average method)
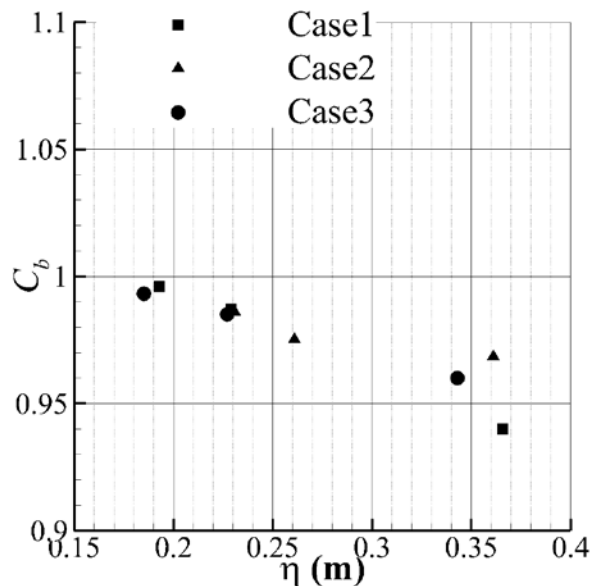

Figure 10. Relationship between the average rate of reduction and overflow height

d) Relationship with the bearing capacity failure

At least, as shown by the video, in Case 1 and Case 2, no failure line of the bearing capacity was seen, and in case 3 with a small quantity of riprap, after the caisson was slightly displaced horizontally, a failure line appeared inside the foundation mound. On the other hand, as shown in Table 2, the sliding safety factor does not change in both case 2 and case 3, so it is assumed that after the caisson slid, the foundation mound failed.

Tensile test in the atmosphere

a) Test method and conditions

Tensile testing was done in the atmosphere in order to confirm the friction coefficient. A foundation mound was built in the atmosphere and at a location about 1/3 below the height of the caisson, it was pulled with a winch. It was done to both the rectangular and the trapezoidal caissons, and in order to see its relationship with scouring, it was compared with a case where joint scouring and overflow scouring were excavated in advance. Each case is shown in Table 3. The percentages in the table are, in the case of joint scouring, percentages of the caisson width equal to the width of the joint, and the percentages of the width combining both ends (see left side of Fig. 11.) The percentages of the overflow scouring width are ratios to the caisson length (direction pulled), and excavation is done across the entire bottom (see right side of Fig. 11.). Photo 7. shows an example of the initial state when it was done forming scouring.

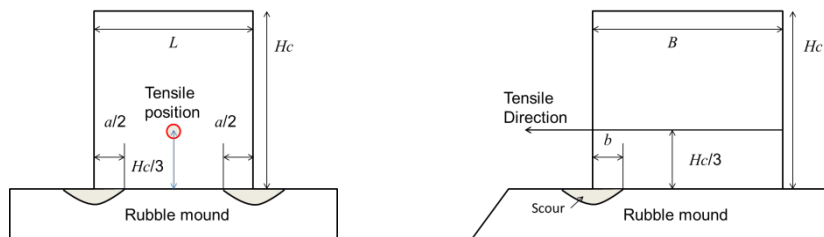| Table 3. Experimental Conditions of tensile test			
Type of Caisson	Ratio of Joint flow Scour to caisson width (*a*/**L**)	Ratio of Overflow Scour to caisson length (*b*/*B*)	Size of rubble
Rectangle	0%	0%	3 and 6
	20%, 30%, 40%	0%	3
	0%	10%, 20%	3
Trapezoid	0%	0%	3 and 6

Figure 11. Image of Joint flow scour (left) and overflow scour (right)

Photo 7. Initial state (left: Ratio of Joint flow Scour 30%, right Ratio of Overflow Scour 20%)

b) Test results

Figure 12 shows the results of performing each three times. It was organized as the friction coefficient when, after being stable for a few centimeters, it started to move. It is assumed that because it moved very slowly, it is not a coefficient of dynamic friction. The friction coefficient itself is presumed to not depend on the installation surface area, but if the scouring width was increased, the friction coefficient changed, so it was organized as the apparent friction coefficient. The mechanism should probably be studied in detail in the future. The results are the average shown in white. It was done from 3 to 4 times, and the block spots represent each time, while the white spots represent the

averages. Examining this shows that the apparent friction coefficient is also impacted by the joint scouring width, but that it is impacted even more by the overflow scouring width, which declines about 25%, even at 10%.
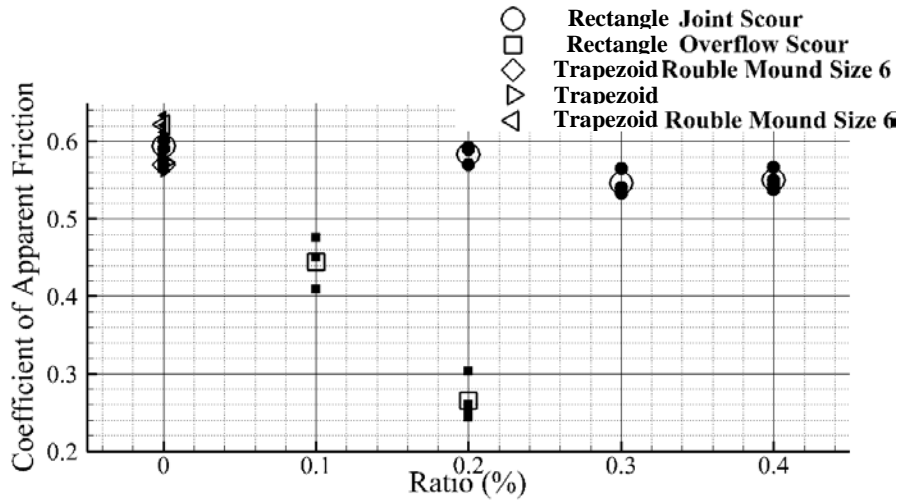

Figure 12. Relation between coefficient of apparent friction and scour ratio

NUMERICAL EXPERIMENT

Numerical Calculation Conditions

The calculation was done Using CADMAS-SURF/3D (CDIT, 2012), dividing the computational grid into 5cm grids, and assuming the same size as the channel, the joints were given as grids with void ratio of 50%. The foundation mound was impermeable. The caisson models were rectangular and trapezoidal, the initial water level was 3.85m, and the flow velocity of the inflow/discharge boundary was set for 8 cases: 0.025, 0.05, 0.075, 0.100, 0.125, 0.150, 0.175, 0.20 m/s.

Computation results

a) State of the computation

Fig. 13. shows one example using a rectangular caisson, where the water level gradually changed from the initial water level (discharge/inflow 0.1m/s). This shows that it is possible calculate the same situation as that in Photo 1.

Fig. 14. shows the rectangular model at 0.1m/s case. Because the caisson slid in the experiment near 65s, the computation was greatly displaced, but it shows that in this area, the water level and wave pressure of the calculation and experiment conformed. Turning to the trapezoid, it conformed with the 0.125m/s case.
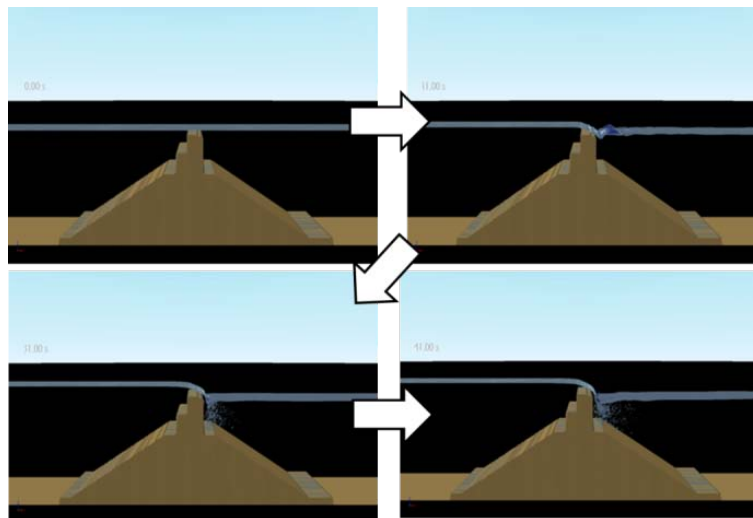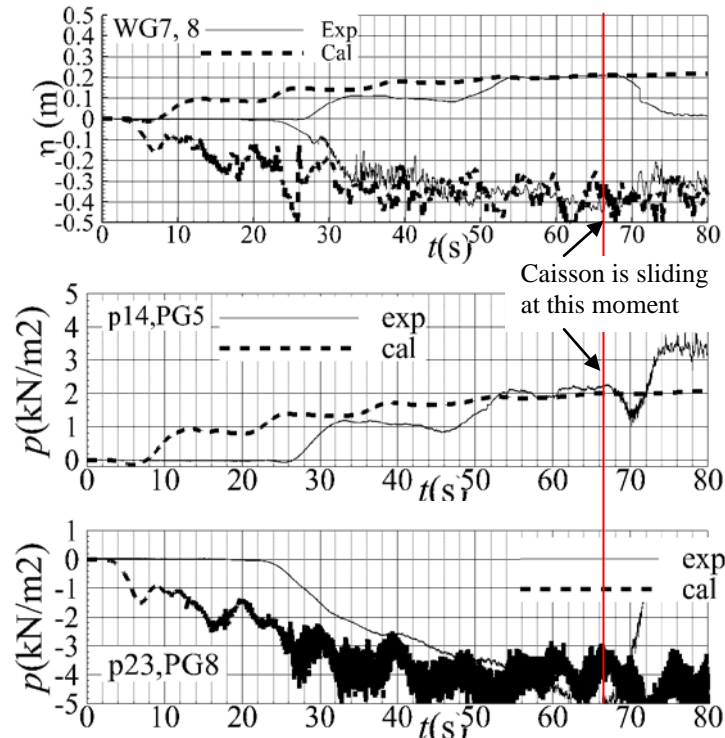

Figure 13. State of calculation

Figure 14. Time history comparison with the experimental results at WG7, WG8, PG5 and PG8

b) Back surface wave pressure reduction rate

In Fig. 15. the water level of the front surface of the caisson is η_f, the water level at the back surface is η_b, the distance from the foundation mound to the back surface water level is h_b, and the ratio of the water level difference and at the front surface and back surface (η_f- η_b) and h_b is considered to be the water level difference/back surface water level ratio.
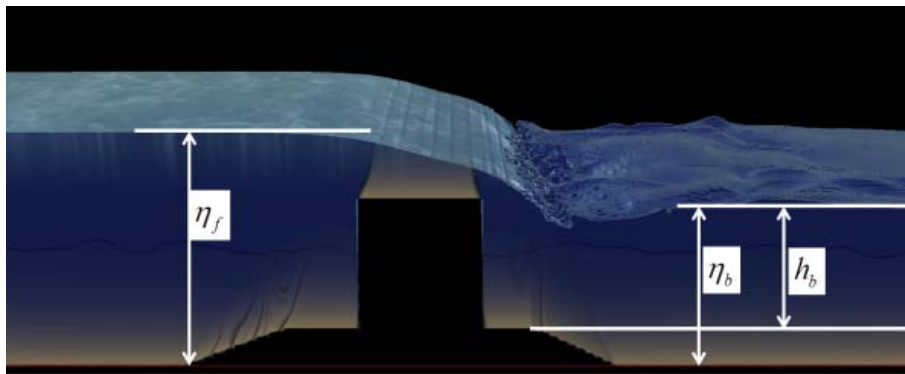

Figure 15. Definition of water level

Fig. 16. plots the relationship between the water level difference/back surface water level ratio and reduction rate (C_b) at the time when the reduction rate was lowest, based on time history data of the reduction rate and water level difference/back surface water level ratio in each case. Black shows the experimental results and white shows the calculation results.
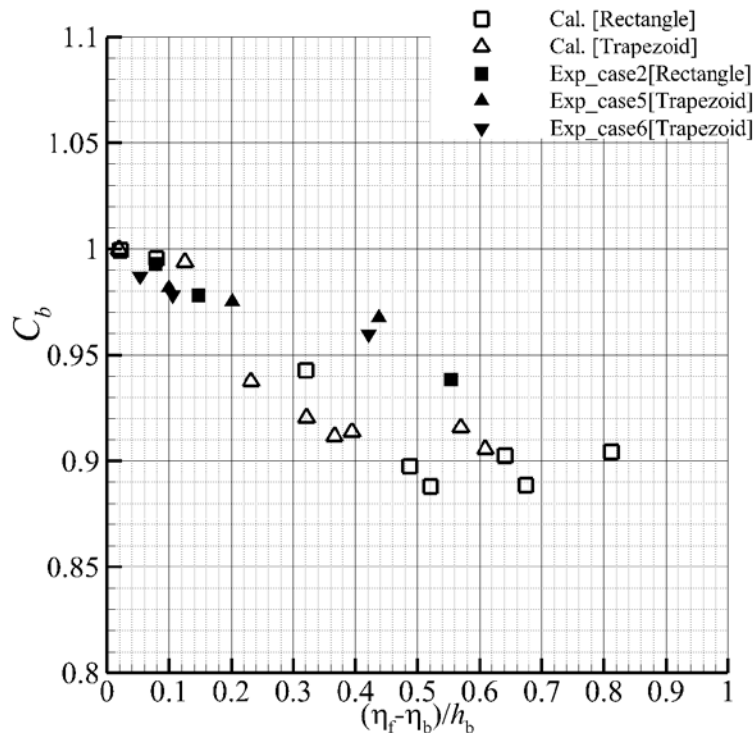
Figure 16. Relation between the rate of reduction and water level difference

Although overall they conform, if the water level difference/back surface water level ratio increases, the numerical calculation obtains C_b smaller than that obtained by the experiments. This means that because the disturbance of the pressure fluctuation behind the caisson is larger in the calculation results, it is presumed that the overflow water mass splashed down nearer the back surface than in the experiment, and that its impact is one cause.

This shows that on the other hand, when the water level difference/back surface water level ratio was large, the reduction rate was not necessarily at its minimum value. This is a result of the fact that if the water level difference/back surface water level ratio is large, the overflow velocity rises, and the splash down location is far from the back surface, so the impact on the back surface water pressure is reduced. Judging from these results, in the Kamaishi case, the reduction rate is a minimum of about 11%.

SUMMARY

Using a 1/20 scale model to model Kamaishi, we studied the stability of the breakwater during tsunami overflow. The results have revealed that the rate of reduction from the hydrostatic pressure at the back surface could be about 10%, and the overflow scouring has a particularly great impact on the apparent friction coefficient. Also based on past research results, we assume that the major cause of the collapse of the breakwater at the Kamaishi Harbor mouth is the water level difference, and that the fall of the back surface pressure during overflow and rise of instability of the mound by scouring made them more vulnerable to collapse at the same time as it scattered their collapse.

REFERENCES

Arikawa, T., M. Sato, K. Shimosako, T. Tomita, D. Tatsumi, Y. Gyoeng-Seon, K. Takahashi (2012): Study of the mechanism of tsunami damage to breakwaters at the mouth of Kamaishi Harbor — First report focused on hydraulic properties—, Document of the Port and Airport Research Institute, No. 1251, 52p

Coastal Development Institute of Technology (CDIT): Research and development of the CADMAS－SURF/3D Numerical Wave Flume, Coastal Technology Library, No. 39

Kobayashi, M., M. Terashi, K. Takahashi, K. Nakajima, T. Kotani (1987): New calculation method for riprap mounds, Report by the Port and Airport Research Institute, Vol. 26, No.(1), pp. 371-412.

Takahashi, S., et. al. (34)(2011): Early report on the survey of earthquake and tsunami damage to ports, coastlines, and airports by the Great East Japan Earthquake of 2011, Document of the Port and Airport Research Institute, No. 1231, 200p

Tanimoto, K., T. Takayama, K. Murakami, S. Murata, H. Tsuruya, S. Takahashi, M. Morikawa, Y. Yoshimoto, S. Nakano, T. Hiraishi (1983): Brief consideration of the actual state of the Japan Sea Chubu Earthquake Tsunami of 1983, Document of the Port and Airport Research Institute, No. 0470, 200p

Horiguchi, T., M. Yokota (1968): Report on the survey of the Tokachi Offshore Earthquake Tsunami, Proceedings of the 15th Conference on Coastal Engineering, pp. 243-253